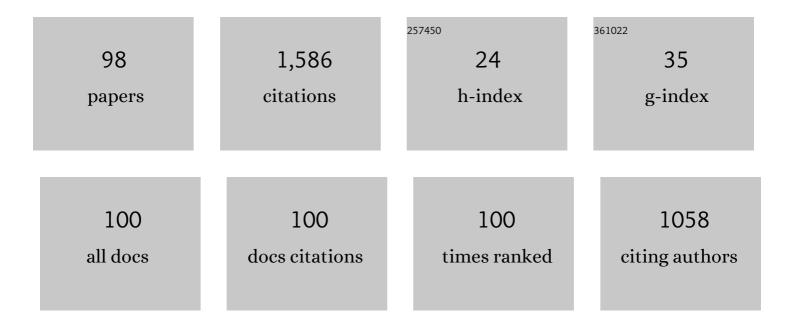
Yubin Zhang

List of Publications by Year in descending order

Source: https://exaly.com/author-pdf/5698430/publications.pdf Version: 2024-02-01



#	Article	IF	CITATIONS
1	Extension twin variant selection during uniaxial compression of a magnesium alloy. Materials Science & Engineering A: Structural Materials: Properties, Microstructure and Processing, 2012, 550, 138-145.	5.6	62
2	Enhanced strength in pure Ti via design of alternating coarse- and fine-grain layers. Acta Materialia, 2021, 206, 116627.	7.9	62
3	Grain boundary mobilities in polycrystals. Acta Materialia, 2020, 191, 211-220.	7.9	61
4	Phase-field simulation study of the migration of recrystallization boundaries. Physical Review B, 2013, 88, .	3.2	60
5	Three-dimensional investigation of recrystallization nucleation in a particle-containing Al alloy. Scripta Materialia, 2012, 67, 320-323.	5.2	57
6	Observations of orientation dependence of surface morphology in tungsten implanted by low energy and high flux D plasma. Journal of Nuclear Materials, 2013, 443, 452-457.	2.7	55
7	Analysis of the growth of individual grains during recrystallization in pure nickel. Acta Materialia, 2009, 57, 2631-2639.	7.9	52
8	Local boundary migration during recrystallization in pure aluminium. Scripta Materialia, 2011, 64, 331-334.	5.2	49
9	Three-dimensional grain growth in pure iron. Part I. statistics on the grain level. Acta Materialia, 2018, 156, 76-85.	7.9	48
10	Effects of heterogeneity on recrystallization kinetics of nanocrystalline copper prepared by dynamic plastic deformation. Acta Materialia, 2014, 72, 252-261.	7.9	47
11	Oriented growth during recrystallization revisited in three dimensions. Scripta Materialia, 2014, 72-73, 9-12.	5.2	43
12	Ultra-low-angle boundary networks within recrystallizing grains. Scripta Materialia, 2017, 139, 87-91.	5.2	36
13	Annealing behaviour of a nanostructured Cu–45Âat.%Ni alloy. Journal of Materials Science, 2013, 48, 4183-4190.	3.7	35
14	Microstructure and mechanical properties of nickel processed by accumulative roll bonding. Materials Science & Engineering A: Structural Materials: Properties, Microstructure and Processing, 2013, 576, 160-166.	5.6	34
15	Effects of spark plasma sintering conditions on the anisotropic thermoelectric properties of bismuth antimony telluride. RSC Advances, 2016, 6, 59565-59573.	3.6	33
16	Three-dimensional local residual stress and orientation gradients near graphite nodules in ductile cast iron. Acta Materialia, 2016, 121, 173-180.	7.9	32
17	A method to correct coordinate distortion in EBSD maps. Materials Characterization, 2014, 96, 158-165.	4.4	31
18	The influence of multiscale heterogeneity on recrystallization in nickel processed by accumulative roll bonding. Journal of Materials Science, 2017, 52, 2730-2745.	3.7	28

#	Article	IF	CITATIONS
19	Cryogenic toughness in a low-cost austenitic steel. Communications Materials, 2021, 2, .	6.9	28
20	Microstructural characterization of nickel subjected to dynamic plastic deformation. Scripta Materialia, 2012, 66, 335-338.	5.2	27
21	In-situ synchrotron X-ray micro-diffraction investigation of ultra-low-strain deformation microstructure in laminated Ti-Al composites. Acta Materialia, 2021, 202, 149-158.	7.9	27
22	In-Situ Investigation of Local Boundary Migration During Recrystallization. Metallurgical and Materials Transactions A: Physical Metallurgy and Materials Science, 2014, 45, 2899-2905.	2.2	26
23	Microstructure and residual elastic strain at graphite nodules in ductile cast iron analyzed by synchrotron X-ray microdiffraction. Acta Materialia, 2019, 167, 221-230.	7.9	26
24	Evolution of microstructure and mechanical properties during annealing of heavily rolled AlCoCrFeNi2.1 eutectic high-entropy alloy. Materials Science & Engineering A: Structural Materials: Properties, Microstructure and Processing, 2022, 833, 142558.	5.6	26
25	Impact of micro-scale residual stress on in-situ tensile testing of ductile cast iron: Digital volume correlation vs. model with fully resolved microstructure vs. periodic unit cell. Journal of the Mechanics and Physics of Solids, 2019, 125, 714-735.	4.8	25
26	Direct Observation of Grain Boundary Migration during Recrystallization within the Bulk of a Moderately Deformed Aluminium Single Crystal. Materials Transactions, 2014, 55, 128-136.	1.2	24
27	Direct observation of nucleation in the bulk of an opaque sample. Scientific Reports, 2017, 7, 42508.	3.3	23
28	Microstructure and strengthening mechanisms of 90W–7Ni–3Fe alloys prepared using laser melting deposition. Journal of Alloys and Compounds, 2020, 838, 155545.	5.5	23
29	In-situ investigation of the evolution of annealing twins in high purity aluminium. Scripta Materialia, 2018, 153, 68-72.	5.2	21
30	Importance of Non-uniform Boundary Migration for Recrystallization Kinetics. Metallurgical and Materials Transactions A: Physical Metallurgy and Materials Science, 2018, 49, 5246-5258.	2.2	21
31	Microstructural characterization of eutectic and near-eutectic AlCoCrFeNi high-entropy alloys. Journal of Alloys and Compounds, 2020, 822, 153558.	5.5	21
32	Analysis of the correlation between micro-mechanical fields and fatigue crack propagation path in nodular cast iron. Acta Materialia, 2020, 188, 302-314.	7.9	21
33	Analysis of through-thickness heterogeneities of microstructure and texture in nickel after accumulative roll bonding. Journal of Materials Science, 2014, 49, 287-293.	3.7	20
34	Microstructural Analysis of Orientation-Dependent Recovery and Recrystallization in a Modified 9Cr-1Mo Steel Deformed by Compression at a High Strain Rate. Metallurgical and Materials Transactions A: Physical Metallurgy and Materials Science, 2016, 47, 4682-4693.	2.2	19
35	Boundary migration in a 3D deformed microstructure inside an opaque sample. Scientific Reports, 2017, 7, 4423.	3.3	19
36	High Resolution Mapping of Orientation and Strain Gradients in Metals by Synchrotron 3D X-ray Laue Microdiffraction. Quantum Beam Science, 2019, 3, 6.	1.2	18

#	Article	IF	CITATIONS
37	3D characterization of partially recrystallized Al using high resolution diffraction contrast tomography. Scripta Materialia, 2018, 157, 72-75.	5.2	17
38	Particle stimulated nucleation revisited in three dimensions: a laboratory-based multimodal X-ray tomography investigation. Materials Research Letters, 2021, 9, 65-70.	8.7	15
39	Importance of Local Structural Variations on Recrystallization. Materials Science Forum, 2013, 753, 37-41.	0.3	13
40	Local residual stresses and microstructure within recrystallizing grains in iron. Materials Characterization, 2022, 191, 112113.	4.4	13
41	Supercube grains leading to a strong cube texture and a broad grain size distribution after recrystallization. Philosophical Magazine, 2015, 95, 2427-2449.	1.6	12
42	4D Study of Grain Growth in Armco Iron Using Laboratory X-ray Diffraction Contrast Tomography. IOP Conference Series: Materials Science and Engineering, 2017, 219, 012039.	0.6	12
43	Impact of 3D/4D methods on the understanding of recrystallization. Current Opinion in Solid State and Materials Science, 2020, 24, 100821.	11.5	12
44	Influence of geometrical alignment of the deformation microstructure on local migration of grain boundaries during recrystallization: A phase-field study. Scripta Materialia, 2021, 191, 116-119.	5.2	12
45	Improved grain mapping by laboratory X-ray diffraction contrast tomography. IUCrJ, 2021, 8, 559-573.	2.2	12
46	Importance of deformation-induced local orientation distributions for nucleation of recrystallisation. Acta Materialia, 2021, 210, 116808.	7.9	12
47	A flexible and standalone forward simulation model for laboratory X-ray diffraction contrast tomography. Acta Crystallographica Section A: Foundations and Advances, 2020, 76, 652-663.	0.1	12
48	Micromechanical impact of solidification regions in ductile iron revealed via a 3D strain partitioning analysis method. Scripta Materialia, 2020, 178, 463-467.	5.2	11
49	Optimizing laboratory X-ray diffraction contrast tomography for grain structure characterization of pure iron. Journal of Applied Crystallography, 2021, 54, 99-110.	4.5	11
50	A phase-field simulation study of irregular grain boundary migration during recrystallization. IOP Conference Series: Materials Science and Engineering, 2015, 89, 012037.	0.6	10
51	Stored energy and recrystallized microstructures in nickel processed by accumulative roll bonding to different strains. Materials Characterization, 2017, 129, 323-328.	4.4	10
52	Crack formation within a Hadfield manganese steel crossing nose. Wear, 2019, 438-439, 203049.	3.1	9
53	Quantification of local dislocation density using 3D synchrotron monochromatic X-ray microdiffraction. Materials Research Letters, 2021, 9, 182-188.	8.7	9
54	Effects of dislocation boundary spacings and stored energy on boundary migration during recrystallization: A phase-field analysis. Acta Materialia, 2021, 221, 117377.	7.9	9

#	Article	IF	CITATIONS
55	Quantification of microstructure in a eutectic high entropy alloy AlCoCrFeNi _{2.1} . IOP Conference Series: Materials Science and Engineering, 2019, 580, 012039.	0.6	8
56	An experimentally-based molecular dynamics analysis of grain boundary migration during recrystallization in aluminum. Scripta Materialia, 2022, 211, 114489.	5.2	8
57	Investigation of boundary migration during grain growth in fully recrystallised high purity nickel. Materials Science and Technology, 2010, 26, 197-202.	1.6	7
58	Crystallographic Analysis of Nucleation at Hardness Indentations in High-Purity Aluminum. Metallurgical and Materials Transactions A: Physical Metallurgy and Materials Science, 2016, 47, 5863-5870.	2.2	7
59	Recrystallization boundary migration in the 3D heterogeneous microstructure near a hardness indent. Scripta Materialia, 2021, 205, 114187.	5.2	7
60	An electron microscopy study of microstructural evolution during in-situ annealing of heavily deformed nickel. Materials Letters, 2017, 186, 102-104.	2.6	6
61	Dislocation density in fine grain-size spark-plasma sintered aluminum measured using high brightness synchrotron radiation. Materials Letters, 2020, 269, 127653.	2.6	6
62	Kinetics of Thermal Grooving during Low Temperature Recrystallization of Pure Aluminum. Materials Science Forum, 2013, 753, 117-120.	0.3	5
63	Damage evolution around white etching layer during uniaxial loading. Fatigue and Fracture of Engineering Materials and Structures, 2020, 43, 201-208.	3.4	5
64	Unsupervised Deep Learning for Laboratory-Based Diffraction Contrast Tomography. Integrating Materials and Manufacturing Innovation, 2020, 9, 315-321.	2.6	5
65	Deep learning for improving non-destructive grain mapping in 3D. IUCrJ, 2021, 8, 719-731.	2.2	5
66	Twinning during recrystallization and its correlation with the deformation microstructure. Scripta Materialia, 2022, 219, 114852.	5.2	5
67	Quantification of room temperature strengthening of laser shock peened Ni-based superalloy using synchrotron microdiffraction. Materials and Design, 2022, 221, 110948.	7.0	5
68	Boundary Fractal Analysis of Two Cube-oriented Grains in Partly Recrystallized Copper. IOP Conference Series: Materials Science and Engineering, 2015, 82, 012006.	0.6	4
69	Roughness of grain boundaries in partly recrystallized aluminum. Scripta Materialia, 2017, 126, 45-49.	5.2	4
70	Boundary migration during recrystallization: experimental observations. IOP Conference Series: Materials Science and Engineering, 2015, 89, 012015.	0.6	3
71	Quantification of deformation microstructure at ultra-low tensile strain in pure Al prepared by spark plasma sintering. IOP Conference Series: Materials Science and Engineering, 2017, 219, 012050.	0.6	3
72	Quantification of local mobilities. Scripta Materialia, 2018, 146, 286-289.	5.2	3

#	Article	IF	CITATIONS
73	Aging of 3D-printed maraging steel. IOP Conference Series: Materials Science and Engineering, 2019, 580, 012047.	0.6	3
74	Quantification of local boundary migration in 2D/3D. IOP Conference Series: Materials Science and Engineering, 2019, 580, 012015.	0.6	3
75	Interface engineering of functionally graded steel-steel composites by laser powder bed fusion. Manufacturing Letters, 2021, 28, 46-49.	2.2	3
76	Microstructure Evolution and Tensile Properties of Cold-Rolled and Annealed Fe-30Mn-0.14C-7Cr-0.26Ni Steel. Metallurgical and Materials Transactions A: Physical Metallurgy and Materials Science, 2021, 52, 3839-3848.	2.2	3
77	Dark field X-ray microscopy for studies of recrystallization. IOP Conference Series: Materials Science and Engineering, 2015, 89, 012016.	0.6	2
78	36th RisÃ, International Symposium on Materials Science. IOP Conference Series: Materials Science and Engineering, 2015, 89, 011001.	0.6	2
79	Kinetics of individual grains during recrystallization of cold-rolled copper. IOP Conference Series: Materials Science and Engineering, 2015, 82, 012048.	0.6	2
80	Recrystallization texture in nickel heavily deformed by accumulative roll bonding. IOP Conference Series: Materials Science and Engineering, 2017, 219, 012034.	0.6	2
81	Synchrotron measurements of local microstructure and residual strains in ductile cast iron. IOP Conference Series: Materials Science and Engineering, 2017, 219, 012054.	0.6	2
82	Alignment of sample position and rotation during <i>in situ</i> synchrotron X-ray micro-diffraction experiments using a Laue cross-correlation approach. Journal of Applied Crystallography, 2019, 52, 1119-1127.	4.5	2
83	In Situ Synchrotron X-ray Micro-Diffraction Investigation of Elastic Strains in Laminated Ti-Al Composites. Metals, 2021, 11, 668.	2.3	2
84	3D Characterization of Recrystallization Boundaries. , 2012, , 31-36.		2
85	Residual strain–stress in manganese steel railway crossing determined by synchrotron and laboratory X-rays. Materials Science and Technology, 2021, 37, 6-13.	1.6	2
86	Three-dimensional grain resolved strain mapping using laboratory X-ray diffraction contrast tomography: theoretical analysis. Journal of Applied Crystallography, 2022, 55, 21-32.	4.5	2
87	Effects of structural heterogeneity of nanostructured copper on the evolution of the sizes of recrystallized grains during annealing. IOP Conference Series: Materials Science and Engineering, 2015, 89, 012033.	0.6	1
88	Nucleation at hardness indentations in cold rolled Al. IOP Conference Series: Materials Science and Engineering, 2015, 89, 012054.	0.6	1
89	Local strain distributions in partially recrystallized copper determined by in situ tensile investigation. IOP Conference Series: Materials Science and Engineering, 2015, 82, 012103.	0.6	1
90	Characterization of boundary roughness of two cube grains in partly recrystallized copper. IOP Conference Series: Materials Science and Engineering, 2015, 89, 012044.	0.6	1

#	Article	IF	CITATIONS
91	Structural coarsening during annealing of an aluminum plate heavily deformed using ECAE. IOP Conference Series: Materials Science and Engineering, 2015, 89, 012035.	0.6	1
92	A method to characterize the roughness of 2â€Ð line features: recrystallization boundaries. Journal of Microscopy, 2017, 265, 313-321.	1.8	1
93	Investigation of plastic yielding in near-micrometer grain size aluminum using synchrotron microdiffraction. IOP Conference Series: Materials Science and Engineering, 2019, 580, 012056.	0.6	1
94	Orientations of recrystallization nuclei developed in columnar-grained Ni at triple junctions. IOP Conference Series: Materials Science and Engineering, 2015, 82, 012044.	0.6	0
95	Thermal stability of laser shock peening processed Ni-based superalloy DZ17G. IOP Conference Series: Materials Science and Engineering, 2019, 580, 012059.	0.6	Ο
96	Impact of local Si segregation on strain localization in ductile cast iron. IOP Conference Series: Materials Science and Engineering, 2020, 861, 012038.	0.6	0
97	Recent trends in Xâ€rayâ€based characterization of nodular cast iron. Material Design and Processing Communications, 2021, 3, e212.	0.9	0
98	3D Characterization of Recrystallization Boundaries. , 0, , 31-36.		0